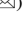# Parametric Study and Finite Element Modelling of Damage-Free Self-centring Column Bases with Different Structural Properties

Elena Elettore[1(✉)] , Fabio Freddi[2] , Massimo Latour[2] ,
and Gianvittorio Rizzano[1]

[1] Department of Civil Engineering, University of Salerno, Salerno, Italy
`eelettore@unisa.it`
[2] Department of Civil, Environmental and Geomatic Engineering,
University College London, London, UK

Abstract. Many recent research studies have focused on the development of innovative seismic-resilient structural systems to reduce repair costs and downtime in the aftermath of severe earthquake events. In this regard, dealing with steel Moment Resisting Frames (MRFs), recent experimental and numerical studies have demonstrated the benefits deriving from the replacement of conventional full-strength column bases (CBs) with innovative damage-free and self-centring CBs, for both damage and residual drifts reductions. Although several technologies have been conceived, studied, and experimentally tested in this direction, only a few research studies investigated the significant properties of the connections influencing the self-centring capability of these systems. Focusing on a damage-free self-centring steel CB previously investigated by the authors, the present study performs a parametric analysis to evaluate the influence of some design parameters on the seismic performance of steel Moment Resisting Frames (MRFs). Three CB configurations belonging to different case-study MRFs are investigated. Finite element (FE) models of the CB configurations have been designed and developed in the ABAQUS, considering sixteen different cases for each configuration. The FE analysis confirms the effectiveness of the theoretical design methodology and provides additional insights to improve the design requirements.

Keywords: Finite element analysis · Parametric · Self-centring column bases · Structural properties

1 Introduction

The current seismic design philosophy implemented by modern codes worldwide [*e.g.,* 1] is based on capacity design strategies, according to which structures are conceived to concentrate the seismic damage into specific dissipative zones characterised by high ductility and energy dissipation capacity. Within steel Moment Resisting Frames (MRFs), the traditional approach consists in adopting over-strengthened columns and

weak beams, with full-strength connections, by promoting the concentration of damage at the beams' ends [2]. Besides, column bases (CBs) are conventionally designed as full-strength joints. This philosophy typically leads to the development of plastic hinges in the bottom end of the first storey columns, thus causing significant structural damage and residual drifts after a severe seismic event. To overcome these deficiencies, several research studies are focusing on the development of innovative low-damage and resilient structures [*e.g.,* 3–4], hence reducing the high direct and indirect losses as a consequence of severe seismic events.

In this framework, several research studies have demonstrated that CBs have a fundamental role in the seismic response of steel MRFs [*e.g.,* 5–6], and they must be protected from damage to achieve structural resilience. In fact, many experimental and numerical research works have focused their attention on replacing conventional full-strength CBs with low-damage joints, where dampers, such as friction devices (FDs), represent the dissipative elements of the connections [*e.g.*, 7–9]. However, it has been demonstrated that, although the use of FDs can be an efficient solution to protect the frame components from damage, it does not allow the control of the residual drifts. Further improvements focused on the development of self-centring (SC) CB connections by the inclusion of post-tensioned (PT) bars or strands to control gap-opening mechanisms. These systems demonstrated their potential in achieving damage-free and SC behaviour [*e.g.,* 10–12]. Within this context, Latour *et al.* [14] proposed an innovative rocking column splice joint where the seismic behaviour is controlled by a combination of FDs, providing the energy dissipation capacity and PT bars with disk springs, promoting the SC behaviour of the CB.

Although several technologies have been conceived, studied, and experimentally tested in this direction, only a few research studies investigated the significant properties of the CB connections influencing the SC capability of these systems [*e.g.,* 15]. Focusing on a damage-free SC steel CB previously investigated by the authors through numerical simulations [16, 17], the present study performs a parametric analysis to evaluate the influence of some design parameters on the seismic performance of steel MRFs. Three SC-CB configurations belonging to different case-study MRFs have been designed and investigated. Finite element (FE) models of the SC-CB connections have been developed in the ABAQUS [18], considering sixteen different cases for each configuration. The FE analysis confirms the effectiveness of the theoretical design methodology and provides additional insights to improve the design requirements.

2 Case-Study MRFs Equipped with the SC-CBs

The plans and the elevation views of the selected case-study MRFs are shown in Fig. 1. The first case-study MRF has one bay and 2 storeys, with an interstorey height of 2.40 m. The other two case-study MRFs have 3 bays and 2 and 4 storeys, respectively, with an interstorey height of 3.50 m at the first level and of 3.20 at the other levels. These MRFs are extracted from prototype structures with perimeter seismic-resistant MRFs and internal gravity frames. The design is performed in accordance with the Eurocode 8 provisions [1]. Further information about the design assumptions is

provided in [16]. The indications of the first storey columns' cross-sections and the materials adopted for the design are reported in Table 1.

The damage-free SC-CB connections experimentally tested by Latour *et al.* [14] are considered in this study. Their theoretical moment-rotation hysteretic behaviour is calibrated by analytical equations accounting for the expected forces in each component during the rocking behaviour. The FDs are composed of steel S355 plates, HV 10.9 class bolts and friction pads of 8 mm of thermally sprayed friction metal steel shims. The SC system comprises high-strength PT bars 10.9 class and disk springs special washers DIN 6796, providing the ideal stiffness-resistance combination. The material properties of the SC-CBs are summarised in Table 2.
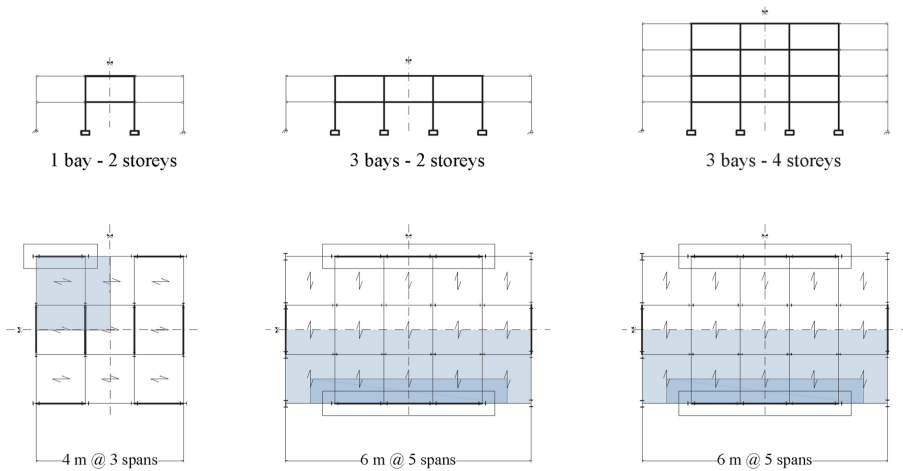
Fig. 1. Plan and elevation view of the case-study buildings

Table 1. Profiles' cross-sections of the first storey columns

Frame	Column's profile	Material
1 bay – 2 storeys	HE 200B	Steel S355
3 bays – 2 storeys	HE 400B	Steel S355
3 bays – 4 storeys	HE 600B	Steel S355

Table 2. Material properties of the SC-CB connections

Column	HE 200B (SC-CB1)	HE 400B (SC-CB2)	HE 600B (SC-CB3)
Web bolts	4 HV M14 (10.9)	4 HV M27 (10.9)	4 HV M30 (10.9)
Flange bolts	4 HV M14 (10.9)	6 HV M27 (10.9)	6 HV M30 (10.9)
PT bars	2 M30 (10.9)	4 M36 (10.9)	6 M36 (10.9)

3 Finite Element Analysis

3.1 Modelling Assumptions

Three detailed 3D nonlinear FE models are developed in ABAQUS [18] to simulate the hysteretic behaviour of the SC-CBs. The results of the models are compared and used to assess the effectiveness of the analytical equations and the design procedure. All the components of the SC-CB are modelled using the eight-node linear brick element (C3D8R) available in the ABAQUS library [18]. Elements C3D8R rely on '*reduced integration*' and '*hourglass control*', and meshing is carried out by selecting local seeds with approximate size 10 in areas with contact interaction and size 15 in the remaining areas. An overview of the model and details of the mesh are shown in Fig. 2. The actual material properties used in the model are those reported in Table 1 and Table 2.

The bottom surface of the base is fully fixed using boundary conditions type '*encastre*', the lateral load is simulated by a controlled horizontal displacement using boundary conditions type '*displacement*', and the gravity load is simulated by a uniform pressure applied at the top surface of the column's cross-section.

To model the initial pre-load force in the web and flange bolts, the option '*bolt load*' is used with the '*apply force*' option keeping the force constant throughout the analysis. Conversely, the initial post-tensioning force in the PT bars is modelled with the '*adjust length*' option to allow capturing the force variation in the PT bars related to the rocking behaviour.
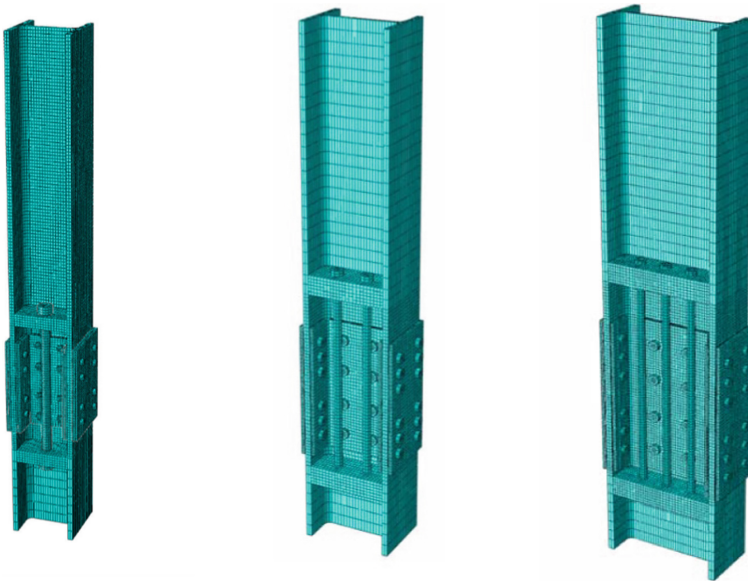

Fig. 2. FE models of the three case-study SC-CBs

The '*surface to surface contact*' is used to model the interaction properties between the parts. This is implemented using the '*hard*' contact property to describe the behaviour in the normal direction, while the '*penalty*' option is used for the tangential response. Friction coefficients equal to 0.30 and 0.53 are used respectively for inter-faces among steel parts (*i.e.,* plates, column, bolts, and PT bars) and for the shims-steel interfaces of the FDs. The options '*specify tolerance for adjustment zone*' is employed to overcome convergence problems associated with the nonlinear nature of the contact regions of bolts and PT bars. The '*TIE*' constraint is used to simulate welding between the anchorage plates of the PT bars and the internal part of the column, both in the upper and lower parts of the column. The nonlinear equilibrium equations are solved using the '*static general*' analysis procedure. The standard '*full Newton*' solution technique is adopted together with an automatic incrementation scheme for the application of the loading. The '*automatic stabilisation*' with '*specify dissipated energy fraction*' is adopted to overcome convergence problems during the analysis.

3.2   Validation Against Experimental Results

The modelling strategy is validated by comparing the response ABAQUS [18] model against the experimental results of the tests carried out by Latour et al. [14]. The experimental campaign included several quasi-static full-scale cyclic tests on the pro-posed damage-free SC-CB connection. The connection was composed of HE 240B sections of S275 steel class, S275 steel plates fastened by M20 HV 10.9 class bolts to both web and flanges, and two M20 threaded bars with disk springs composed by three disks in parallel and seven disks in series. The results of the validation process are shown in Fig. 3. Demonstrating the effectiveness of the FE model in predicting the experimental behaviour. Besides, the current model does not take in account the variation of the pre-loading loss of the web and flange bolts during the experimental test.
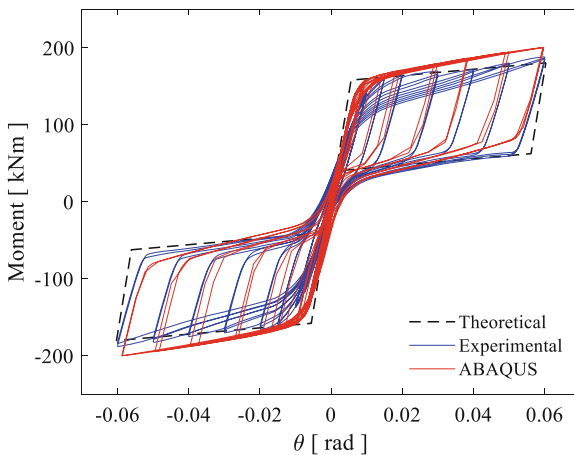

Fig. 3. Validation of the ABAQUS [18] model vs experimental results [14]

4   Parametric FE Analysis

The parametric analysis is carried out to assess the influence of the variation of the following three design properties:

- The thickness of the flanges' plates;
- The design shear load percentage carried by the web FDs;
- The design axial load: the max and min compressive axial force are considered as two limit values for each configuration.

These parameters have been varied, as indicated in Table 1 (Table 3).

Table 3. Matrix parameters for each configuration of the case-study SC-CBs

| Model	Flanges' plate thickness	Shear load % Web FDS	Axial load
Configuration 1	t_1	100	Max (+)-Min (−)
Configuration 2	$2t_1$	100	Max (+)-Min (−)
Configuration 3	t_1	50	Max (+)-Min (−)
Configuration 4	t_1	75	Max (+)-Min (−)
Configuration 5	t_1	0	Max (+)-Min (−)
Configuration 6	$2t_1$	50	Max (+)-Min (−)
Configuration 7	$2t_1$	75	Max (+)-Min (−)
Configuration 8	$2t_1$	0	Max (+)-Min (−)

The preliminary results of the parametric FE analysis have been evaluated in terms of global and local response. For the sake of brevity, in this work, only the local results of the CB with section HE 400B (*i.e.,* SC-CB2) are presented in terms of equivalent plastic strain (PEEQ) distribution. Results show that the global hysteretic behaviour of the SC-CBs is not significantly influenced by the first two parameters (*i.e.,* thickness of the flanges' plates and design shear load percentage), as expected.

Figure 4(a) and (b) show the PEEQ at the end of the cyclic analysis (max drift equal to $\delta = \vartheta_d * l_0 = 64$ mm, where $\vartheta_d = 0.04$ rads is the target rotation and $l_0 = 1600$ mm is the column's length above the splice) for the SC-CB2 in Configurations 1 and 2 and considering the Max compressive axial force. These two configurations are characterised by a thickness of the flanges' plates of 12 mm and 24 mm, respectively. The PEEQ limit has been assumed equal to 0.012, which is the plastic strain of the material. As it can be observed in Fig. 4, increasing the thickness of the flanges' plates leads to an increment of the plastic damage. In fact, the extension of the damage is higher in the Configuration 2 and this is confirmed by observing the amount of dissipated plastic energy (not shown in this paper due to space constraint). Figure 5 shows the maximum strain $\left(\varepsilon_{peak}\right)$ normalized to with respect to the ultimate strain of the material (ε_u), considering the maximum and minimum design axial force. The parameter that has been varied in these two configurations is the design shear load percentage carried by the web FDs (*i.e.,* 100%, 75%, 50%, 0). It is worth highlighting that this parameter has been investigated to evaluate how this design choice affects the

shear redistribution among the different components (*i.e.,* the web FDs, the flange FDs and the sliding mechanisms of the friction at the rocking interface. Preliminary results suggest that designing the web FD to carry 50% of the design shear load leads to a reduction of the damage on the column, as observed in Fig. 5.
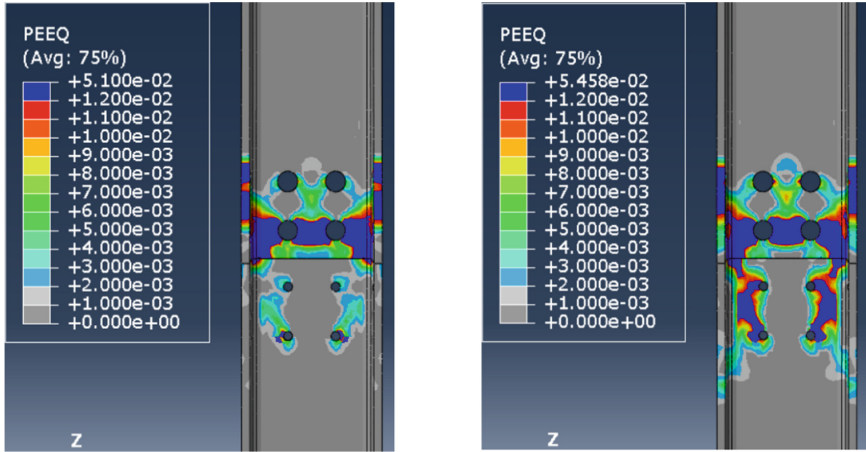
Fig. 4. Influence of the thickness of the flanges' plates. Equivalent plastic strain (PEEQ) distribution at the end of the cyclic analysis of the SC-CB 2: (a) 12 mm; (b) 24 mm.
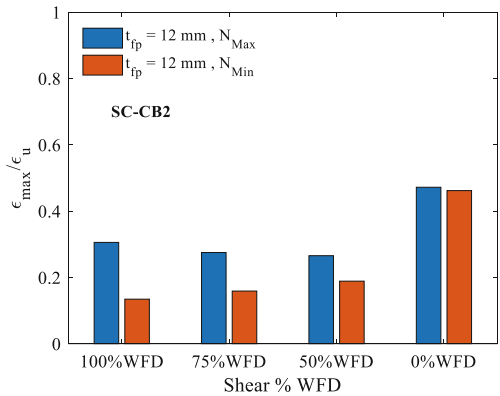
Fig. 5. Influence of the design shear load. Results for the SC-CB 2.

5   Conclusions

The FE model correctly predicts the overall response of the connections observed during the tests. Moreover, the preliminary results of the FE parametric analysis show that the global hysteretic behaviour is not affected by the considered design parameters, while the local behaviour is significantly influenced. Some recommendations are provided to improve the design requirements.

References

1. EN 1998-1 (2004) Eurocode 8: Design of structures for earthquake resistance – Part 1: General rules, seismic actions and rules for buildings, European Committee for Standardization, Brussels
2. Mazzolani FM, Piluso V (1996) Theory and Design of Seismic Resistant Steel Frames, London, UK
3. MacRae G, Clifton GC (2013) Low damage design of steel structures. In: Steel innovations 2013 workshop, Christchurch, New Zealand, 21–22 Februvary 2013
4. Chancellor NB, Eatherton MR, Roke DA, Akbas T (2014) Self-centering seismic lateral force resisting systems: high performance structures for the city of tomorrow. Buildings 4:520–548
5. Zareian F, Kanvinde AM (2013) Effect of column-base flexibility on the seismic response and safety of steel moment-resisting frames. Earthq Spectra 29:1537–1559
6. Inamasu H, Lignos DG, Kanvinde AM (2017) Effect of column base flexibility on the hysteretic response of wide flange steel columns. In: 3rd huixian international forum earthquake engineering young researcher, 11–12 August 2017
7. Mackinven H, MacRae GA, Pampanin S, Clifton GC, Butterworth J (2007) Generation four steel moment frame joints. In: 8th pacific conference on earthquake engineering, Singapore
8. Chi H, Liu J (2012) Seismic behaviour of PT CB for steel self-centring MRFs. J Constr Steel Res 78:117–130
9. Borzouie J, MacRae GA, Chase JG, Rodgers GW, Clifton GC (2016) Experimental studies on cyclic performance of CB strong axis – aligned asymmetric friction connections. J Struct Eng (ASCE) 142(1):1–10
10. Freddi F, Dimopoulos CA, Karavasilis TL (2017) Rocking damage-free steel CB with friction devices: design procedure and numerical evaluation. Earthq Eng Struct Dyn 46:2281–2300
11. Freddi F, Dimopoulos CA, Karavasilis TL (2020) Experimental evaluation of a rocking damage-free steel CB with friction devices. J Struct Eng 146(10):04020217
12. Kamperidis V, Karavasilis TL, Vasdravellis G (2018) Self-centering steel CB with metallic energy dissipation devices. J Constr Steel Res 149:14–30
13. Latour M, D'Aniello M, Zimbru M, Rizzano G, Piluso V, Landolfo R (2018) Removable friction dampers for low-damage steel beam-to-column joints. Soil Dyn Earthq Eng 115:66–81
14. Latour M, Rizzano G, Santiago A, Da Silva L (2019) Experimental response of a low-yielding, self-centering, rocking CB joint with friction dampers. Soil Dyn Earthq Eng 116:580–592
15. Kamperidis VC, Papavasileiou GS, Kamaris GS, Vasdravellis G (2020) Seismic collapse of self-centering steel MRFs with different column base structural properties. J Constr Steel Res 175:106364
16. Elettore E, Freddi F, Latour M, Rizzano G (2021) Design and analysis of a seismic resilient steel moment resisting frame equipped with damage free self-centring column bases. J Constr Steel Res 179:106543
17. Elettore E, Lettieri A, Freddi F, Latour M, Rizzano G (2021) Performance-based assessment of seismic-resilient steel moment resisting frames equipped with innovative CB connections. Structures 32:1646–1664
18. ABAQUS/Standard and ABAQUS/Explicit (2016) Version 2017. ABAQUS Theory Manual, Dassault Systems